Journal of Solid State Chemistry 183 (2010) 521–526

Contents lists available at ScienceDirect

Journal of Solid State Chemistry

journal homepage: www.elsevier.com/locate/jssc

Synthesis, electronic transport and magnetic properties of $Zr_{1-x}Y_xNiSn$, (x=0–0.25) solid solutions

E.K. Hlil [a,*], Yu. Stadnyk [b], Yu. Gorelenko [b], L. Romaka [b], A. Horyń [b], D. Fruchart [a]

[a] Institut Néel, CNRS-UJF, BP 166, 38042 Grenoble Cedex 9, France
[b] Ivan Franko National University of Lviv, Kyryl and Mephodiy Str., 6, 79005 Lviv, Ukraine

ARTICLE INFO

Article history:
Received 16 August 2009
Received in revised form
7 December 2009
Accepted 12 December 2009
Available online 23 December 2009

Keywords:
Solid solution
Electrical resistivity
Seebeck coefficient
Magnetic susceptibility
Electronic structure calculations

ABSTRACT

The crystal structure of the $Zr_{1-x}Y_xNiSn$ half-Heusler solid solutions is synthesized and their crystal structure is determined. Electrical resistivity and thermoelectric Seebeck coefficient are measured in the 80–380 K temperature range, whereas magnetic susceptibility is measured at 290 K. It is established that substitution of Zr host atoms by *Y* in the ZrNiSn intermetallic semiconductor is equivalent to doping by acceptor impurities. Self-consistent ab initio calculations, based on the full potential local orbital (FPLO) minimum basis method, are performed to investigate the electronic and thermoelectric properties of these alloys. Spin polarized within the framework of the coherent potential approximation (CPA) are included.

1. Introduction

The main task, in this work, is the half-Heusler thermoelectric materials optimization based on the «synthesis–crystal structure–properties» correlation mastery. Development of semiconductor with high electrical conductivity, large Seebeck coefficient value and sufficiently low heat conductivity is necessary to obtain highest thermoelectric *figure of merit* values.

Simultaneous occurrence of suitable thermoelectric parameters values is quite unique phenomenon. As a rule, they are closely interdependent which substantially narrows the possibility to elaborate right materials. Among the semiconducting phases suitable as thermoelectric materials a main place is occupied by the intermetallic semiconductors with the MgAgAs structure type (ST) (so called half-Heusler phases); in particular ZrNiSn compound [1–4].

Many works on intermetallic *Me*NiSn semiconductors (*Me*=Ti, Zr, Hf), reported the resistivity and thermopower temperature dependences and proved that at $T \geq 4.2$ K the electrons were the main charge carriers in these phases. In papers [4,5], for the first time, it was supposed to interpret the semiconducting behavior of the phases with the MgAgAs type of structure as the heavily doped and compensated semiconductors [6]. Replacement of either component in these compounds by another chemical element may be seen as doping of alloy by the neutral, acceptor or donor impurities. Furthermore, it was shown that doping of these type semiconductors by significant amount of the charged impurities (10^{19}–10^{21} cm^{-3}) increases the thermoelectric *figure of merit* value. Therefore, the investigation of the ZrNiSn compound doped with acceptor impurities namely by substitution of Zr ($4d^25s^2$) by Y ($4d^15s^2$) atoms seems to be very interesting.

Here, we present the structure characterization, conductivity and Seebeck coefficient temperature dependences. Static magnetic susceptibility of the $Zr_{1-x}Y_xNiSn$ solid solution alloys is performed as well. In addition, experimental data are compared to theoretical results obtained from electronic density of states (DOS) calculations.

2. Experimental details

Samples with yttrium amount (x=0–0.25) were prepared by arc-melting of the pure constituent metals under pure Ti-guttered argon protective atmosphere. The purity of the elements are Zr-99.96 wt%, Ni-99.99 wt%, Sn-99.99 wt% and Y-99.86 wt%. Homogenizing heat treatment of the ingots was performed in the evacuated silica ampoules at 800 °C for 1000 h followed by quenching in ice water. X-ray phase and structure analyses were carried out using the patterns data collected with the DRON-2.0 M diffractometer (Fe$K\alpha$-radiation). The lattice parameters were calculated from simple indexing of the patterns. The based compound ZrNiSn with MgAgAs type is very known, its crystal structure was investigated before using powder and single crystal

* Corresponding author. Fax: +33 4 76 88 10 38.
E-mail address: hlil@grenoble.cnrs.fr (E.K. Hlil).

0022-4596/$ - see front matter © 2009 Elsevier Inc. All rights reserved.
doi:10.1016/j.jssc.2009.12.009

methods. So, for solid solution only lattice parameters were determined. Resistivity (ρ), Seebeck coefficient (S), referred to pure copper, were measured in the 80–380 K temperature range. Static magnetic susceptibility was measured at room temperature.

3. Electronic structure calculations

Electronic and thermoelectric properties of $Zr_{1-x}Y_xNi$ are investigated by *ab initio* calculations based on the density functional theory. The precise self-consistent full potential local orbital minimum basis (FPLO) method was employed [7,8]. Calculations were processed within the framework of the coherent potential approximation (CPA) which takes the disorder into account. We assumed that the 4*a* (1/2, 1/2, 1/2) and 4*b* (1/4, 1/4, 14) sites occupied by Ni and Sn atoms are perfectly ordered whereas the 4*a* (0, 0, 0) site is taken to be randomly shared by Zr and Y atoms. The calculations were performed with the scalar relativistic version using the Perdew and Wang exchange–correlation potential. The included valence basis states are 4*spd* and 5*sp* of both Zr and Y atoms, 3*spd* and 4*sp* of Ni, as well as 4*spd* and 5*sp* of Sn atom. A reciprocal space mesh containing 72 *k*-points within the irreducible wedge of the Brillouin zone was used to perform the self-consistent calculations.

4. Results and discussion

X-ray phase and structure analyses of the samples of $Zr_{1-x}Y_xNiSn$ solid solution showed that they crystallized in single phased MgAgAs structure, except for the $Zr_{0.90}Y_{0.10}NiSn$ and $Zr_{0.75}Y_{0.25}NiSn$ composition, which contained the insignificant impurities of other phase. The $Zr_{0.90}Y_{0.10}NiSn$ alloy contained much more impurities than the $Zr_{0.75}Y_{0.25}NiSn$ sample. Lattice parameters of all samples were obtained from the powder diffraction data and plotted in Fig. 1 versus yttrium content *x*.

As seen in Fig. 1, the lattice parameter of the $Zr_{1-x}Y_xNiSn$ solid solution alloys increases monotonously as the atoms of less size (r_{Zr}=0.160 nm) are replaced by greater atoms (r_Y=0.180 nm). Taking into account that yttrium in these alloys behaves as an acceptor with respect to zirconium, and probably takes place exactly in the positions of the zirconium atoms. Such replacement implies, from semiconductors theory, introduction of acceptor impurity in the ZrNiSn compound. Thus, the acceptor impurity concentration changes proportionally to the yttrium concentration in the $Zr_{1-x}Y_xNiSn$ alloys.

Temperature dependences of resistivity ln $\rho(1/T)$, plotted in Fig. 2, are typical for the doped semiconductors. Minor Zr substitution by Y (x=0.02) results in a considerable decrease of the resistivity, but the semiconducting-like behavior is still retained. From high- and low-temperature dependences of the ln $\rho(1/T)$ plots, the activation energies ε_1^ρ and ε_3^ρ are determined (Table 1). They correspond to electrons or holes activation from the Fermi level into conduction band and to the hopping conduction, respectively.

Activation energy ε_1^ρ monotonously diminishes with the yttrium content increase in the $Zr_{1-x}Y_xNiSn$ solution while x varies from 0.02 to 0.12. This decrease, accompanied by the residual conductivity decrease (Fig. 3), is undertaken when the Fermi level shifts to the valence band edge for this concentration range. At the higher concentration of the acceptor impurity (x=0.2), low temperature region in ln$\rho(1/T)$ plot show that activation energy disappears, thus the transition of insulator-metal occurs. An extremum on the $\varepsilon_1^\rho(x)$ (x=0.02) does not evidence the non-monotonous change in the Fermi level position,

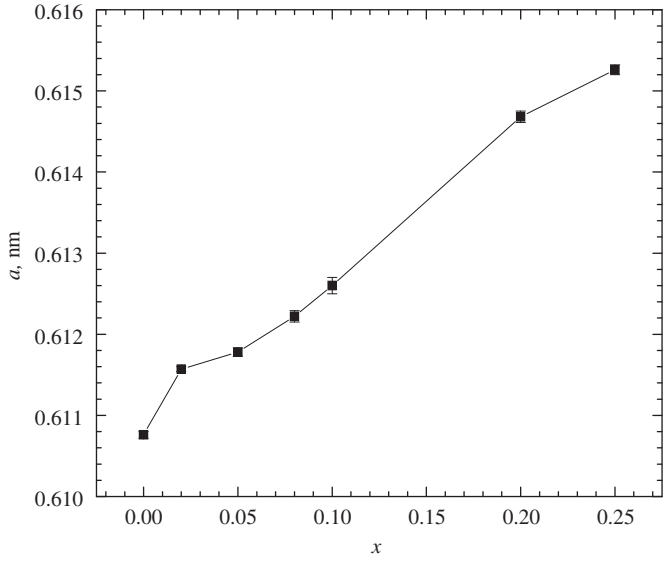

Fig. 1. Dependence of cell parameter a for $Zr_{1-x}Y_xNiSn$ solid solution versus yttrium content. The deviation in lattice parameters is reported for all concentrations but it is visible only for x=0.1 since the deviation for other concentrations is <0.00001.

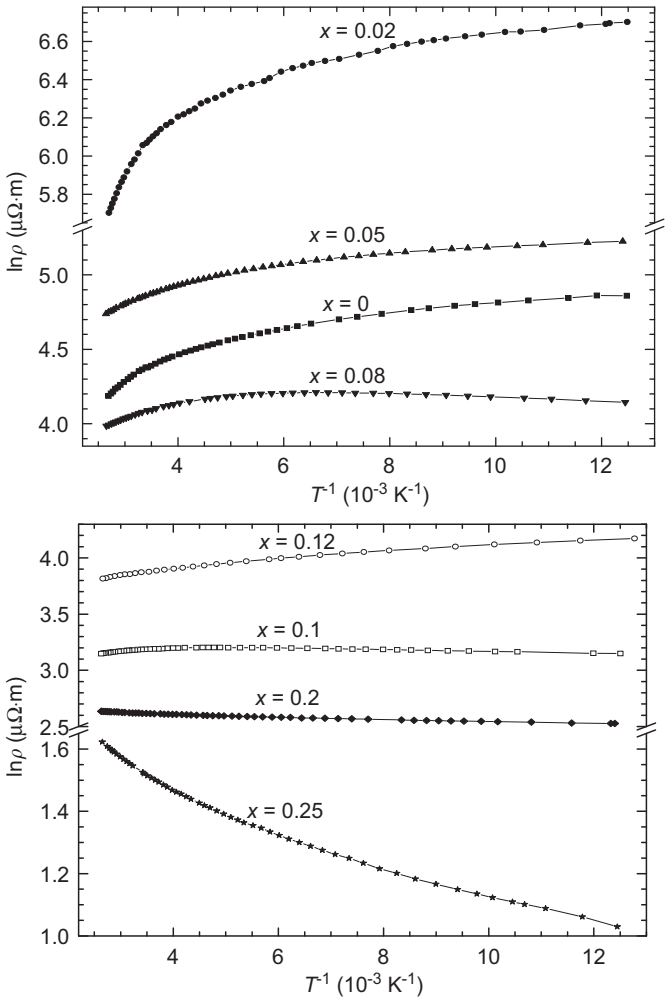

Fig. 2. Temperature dependences of electrical resistivity for $Zr_{1-x}Y_xNiSn$ solid solution alloys.

Table 1
Activation energy and magnetic properties of the $Zr_{1-x}Y_xNiSn$ substitutional solid solution.

Alloy	ε_1^ρ (meV)	ε_3^ρ (meV)	$\chi \times 10^{-6}$ (emu/g)
ZrNiSn	28.90	1.6	0.07 [7]
$Zr_{0.98}Y_{0.02}NiSn$	52.20	2.2	0.077
$Zr_{0.95}Y_{0.05}NiSn$	17.30	1.38	0.148
$Zr_{0.92}Y_{0.08}NiSn$	11.96	–	0.339
$Zr_{0.90}Y_{0.10}NiSn$	–	–	0.621
$Zr_{0.88}Y_{0.12}NiSn$	6.63	–	0.612 [7]
$Zr_{0.80}Y_{0.20}NiSn$	–	–	0.510
$Zr_{0.75}Y_{0.25}NiSn$	–	–	0.590

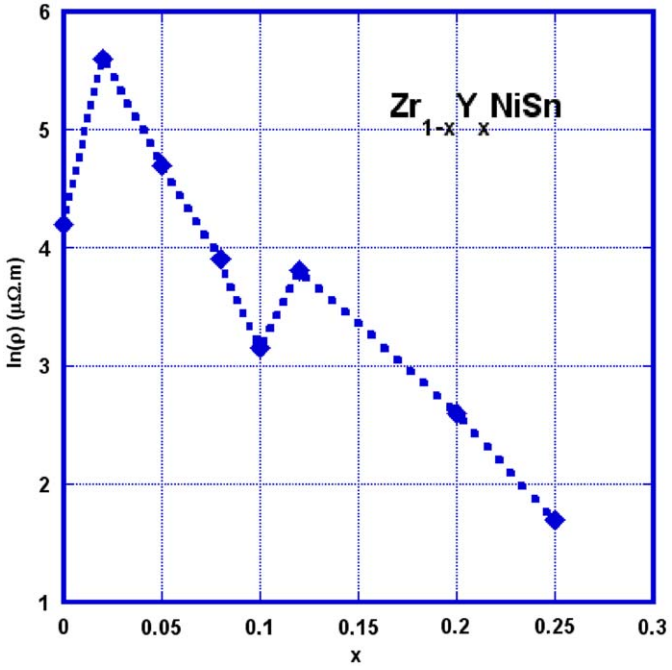

Fig. 3. Composition dependences of residual electrical resistivity for $Zr_{1-x}Y_xNiSn$ solid solution alloys.

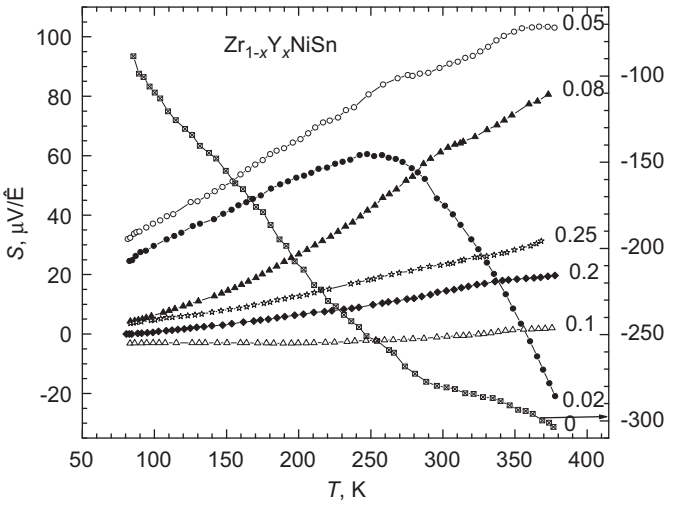

Fig. 4. Temperature dependence of Seebeck coefficient for $Zr_{1-x}Y_xNiSn$ solid solution alloys.

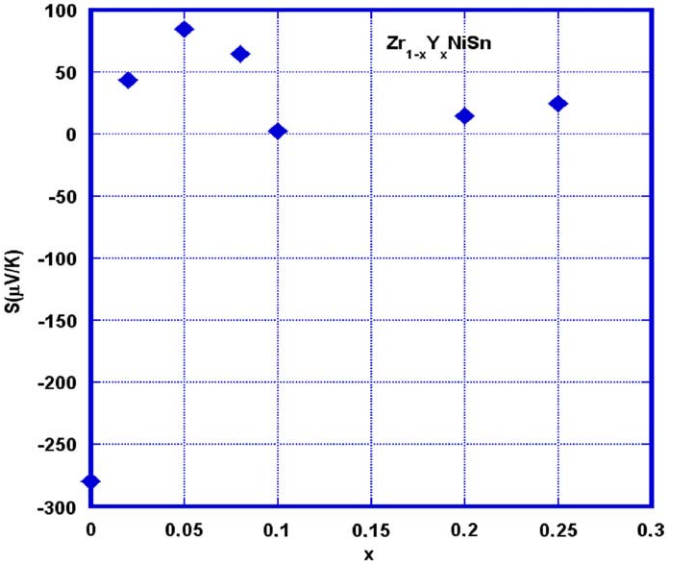

Fig. 5. Compositions dependence of Seebeck coefficient for $Zr_{1-x}Y_xNiSn$ solid solution alloys at T=300 K.

because at x=0, activation of the electrons takes place into the conduction band which is confirmed by the negative sign of the thermopower. Otherwise at $x \geq 0.02$ holes activation into a valence band seems most probable. In other words, inclusion of the yttrium atoms into the crystal structure of the ZrNiSn compound is accompanied by monotonous Fermi level shift to the valence band. Such character of the ε_1^ρ (x) (and proper position of the Fermi level) is the evidence of that the yttrium atoms are disposed strictly in the crystallographic positions of the zirconium atoms. Therefore, the monotonous change of the lattice parameter versus composition of the $Zr_{1-x}Y_xNiSn$ solid solution (Fig. 1) becomes clear.

Thermopower $S(T)$ temperature dependences are presented in Fig. 4. Analysis gives evidence of S sign reverse which indicates a change of the basic current carriers type defining the semiconductor conduction: from electrons in ZrNiSn to holes in $Zr_{1-x}Y_xNiSn$ ($x > 0.02$) type. This change is the result of the parity between concentrations of the controlled acceptor and uncontrolled donor impurities (i.e. the compensation degree). It is possible to assert that at x=0 the Fermi level is situated near the conduction band bottom thus the electrons are the basic charge carriers. For $x \geq 0.02$, the Fermi level approaches to the top of the valence band so that, inversely, the holes become the basic charge carriers and S sign becomes negative. On the other hand, it can be seen in Fig. 4 that the thermopower of the $Zr_{0.90}Y_{0.10}NiSn$ sample has practically a negative value in whole temperature range. Such unexpected behavior of the $S(T)$ dependence can be associated with the presence of impurities in this alloy as it was before mentioned. The uncontrolled donor impurity concentration in the $Zr_{0.90}Y_{0.10}NiSn$ alloy is much more than in other samples of this solid solution. This unexpected result is also evidenced in Fig. 5 (x=0.1) where the S change versus Y content at T=300 K is displayed. Therefore the present concentration of acceptor impurity is insufficient for an overcompensation of the semiconductor and this conclusion is confirmed by the results reported in Figs. 4 and 5, for the close composition of the $Zr_{0.88}Y_{0.12}NiSn$ single phase for which the Seebeck coefficient sign is positive

As in the case of doping of the p-TiCoSb intermetallic semiconductor by the nickel donor impurity [9,10] or doping of the ZrNiSn by the scandium acceptor impurity [11,12], the Anderson transition takes place in $Zr_{1-x}Y_xNiSn$ since $(E_V - E_F) = \Delta E$ value changes its sign while doping impurity content varies [6]. Indeed, at low temperature, $Zr_{1-x}Y_xNiSn$ (x=0) is the compen-

sated semiconductor of electronic type conductivity. At $0.02 \le x \le 0.12$ the Fermi level locates near the top of the valence band and $(E_V - E_F) < 0$. For $x > 0.20$ electrical conductivity is induced by free holes of valence band and $(E_V - E_F) > 0$ since the Fermi level is located in the valence band.

Magnetic susceptibility measurements versus Y content at a room temperature are gathered in Table 1. They evidence a Pauli paramagnets character for $Zr_{1-x}Y_xNiSn$ solid solution samples. As known, the magnetic susceptibility of the Pauli paramagnets is proportional to the density of states at the Fermi level. The increase of χ with increasing acceptor concentration from $x=0$ to 0.12 in the $Zr_{1-x}Y_xNiSn$ alloys is caused by the process of impurity band alteration and the increase of the electronic density of states at the Fermi level as expected from the resistivity and Seebeck coefficient data. Interesting is the greater χ value presence for the $Zr_{0.90}Y_{0.10}NiSn$ alloy in comparison with the $Zr_{0.88}Y_{0.12}NiSn$ which correlates with the unexpected electrophysical properties behavior for $x=0.1$.

In conclusion from the experimental point of view, doping of the ZrNiSn intermetallic semiconductor by the yttrium acceptor impurity leads to the insulator–metal transition of electrical conduction and the inverse of the main charge carriers type. Now, we will be interested in the electronic structure calculations to see how these experimental results will agree with theoretical conclusions.

Total density of states (DOS), deduced from the band structure calculations for all Y concentrations, are presented in Fig. 6a. Firstly, DOS close to the Fermi level displayed in Fig. 6b (inset of Fig. 6a) gives evidence of a small gap presence for ZrNiSn. The gap width is estimated about 0.1 eV, value slightly lower than those calculated by KKR CPA method on this system and previously reported in our works [11]. Taken as a reference, the Fermi level position in the gap induces a zero DOS exhibiting a thermoelectric character, i.e. a semi conducting-like state which correlates the resistivity decrease versus temperature ($d\rho/dT < 0$).

When x increases, the gap disappears and the calculated charge atomic values, found to be insensitive to the Y content, are 39.629, 28.901 and 48.469 for Zr, Ni and Sn, respectively. As expected for alloys, there is practically no charge transfer since these values are slightly different from neutral charge atomic values 40, 28 and 50 for Zr, Ni and Sn isolated atoms, respectively. Projected DOS on atoms, displayed in Fig. 7, specify that total DOS is mainly originating from the 3*d* Ni band contributions in the valence band whereas the *4d* Zr, *4d* Y and *3d* Ni bands contribute to the unoccupied states. DOS contributions, from Sn to both occupied states and unoccupied states, are found weak reference to those of other atoms. The *l*-decomposed DOS of like-states *s*, *p* and *d* (from top to bottom) of Zr, Y, Ni and Sn in $Zr_{0.95}Y_{0.05}NiSn$ solid solution alloys are presented in Fig. 8. They give evidence of the presence of a narrow gap for all atoms like-states *s*. The gap disappearance in total DOS is induced only by like-states *p* and *d* of all atoms except like-states Sn(*d*). It is worth noticing that

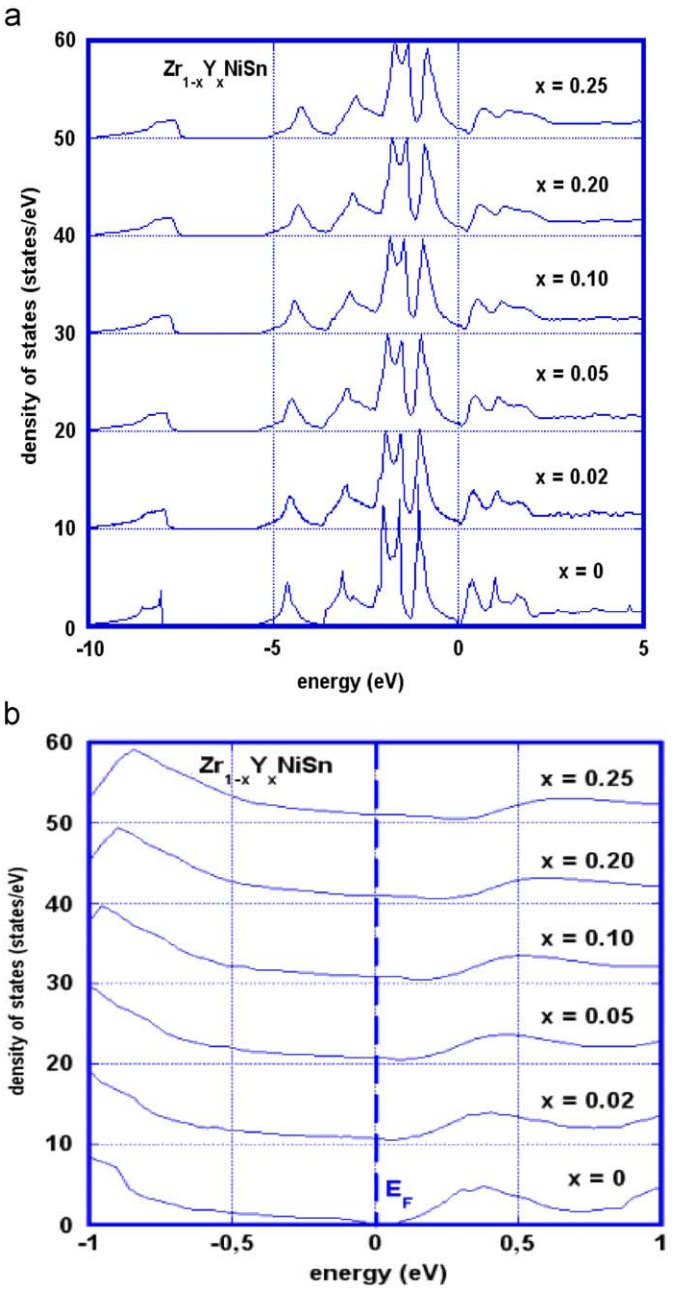

Fig. 6. Total DOS of $Zr_{1-x}Y_xNiSn$ solid solution alloys: (a). The same figure with zoom around Fermi level and (b). For comparison versus concentration, the DOS is shifted on *Y*-axis by 10, 20, 30, 40 and 50 for $x=0.02$, 0.05, 0.10 0.20 and 0.25, respectively.

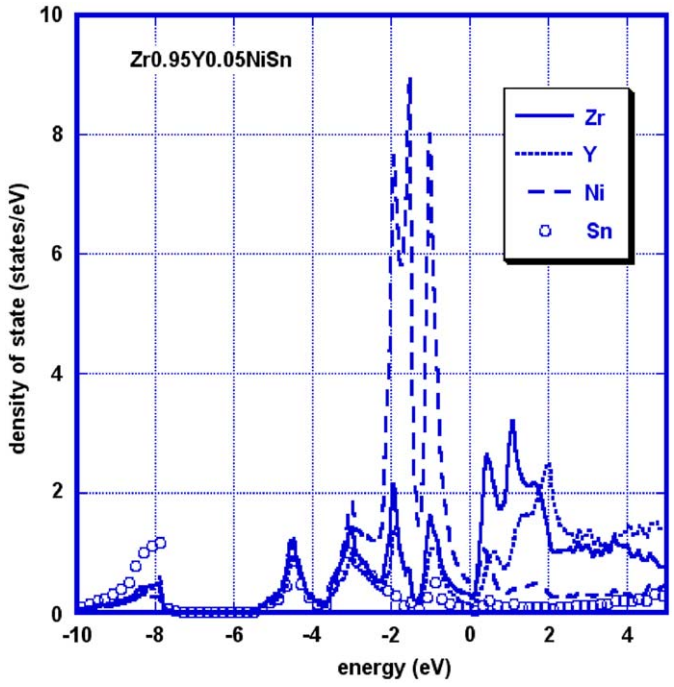

Fig. 7. Projected DOS on Zr, Y, Ni and Sn atoms.

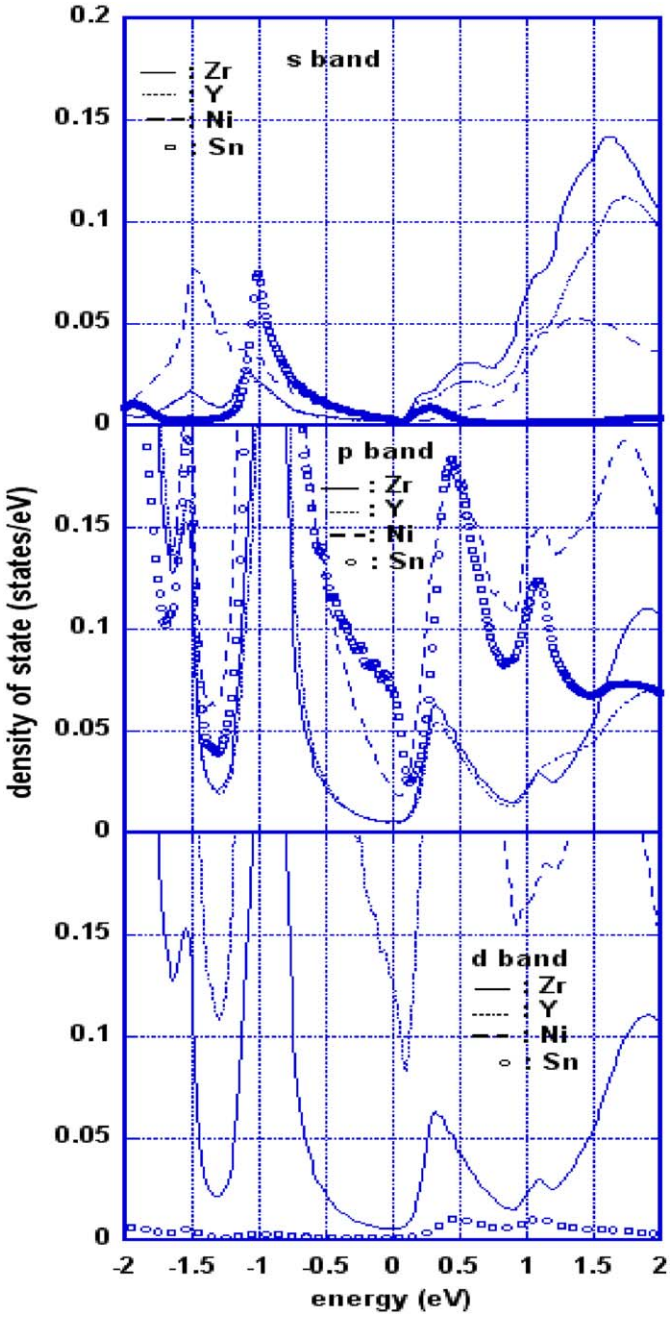

Fig. 8. The *l*-decomposed DOS of like-states *s*, *p* and *d* (from top to bottom) of Zr, Y, Ni and Sn in $Zr_{0.95}Y_{0.05}NiSn$ solid solution alloys.

like-states Sn(*d*) is completely full and the corresponding energy is very deep, consequently they do not contribute to the bonding between atoms.

Calculations confirm the Fermi level shift to the valence band when Zr atom is progressively substituted by Y atom, as expected from our experimental data. This shift is explained in terms of the electron number change in the valence band. Transition from semiconducting-like state (E_F falls in the gap for x=0) to metal-like state (E_F in the BV when x increases) is confirmed as well. As known, this transition involves the Seebeck coefficient value reverse.

Magnetic susceptibility measurement conclusions are also confirmed. Indeed, calculations, performed on perfect samples, point to the increase of the density of states at the Fermi level

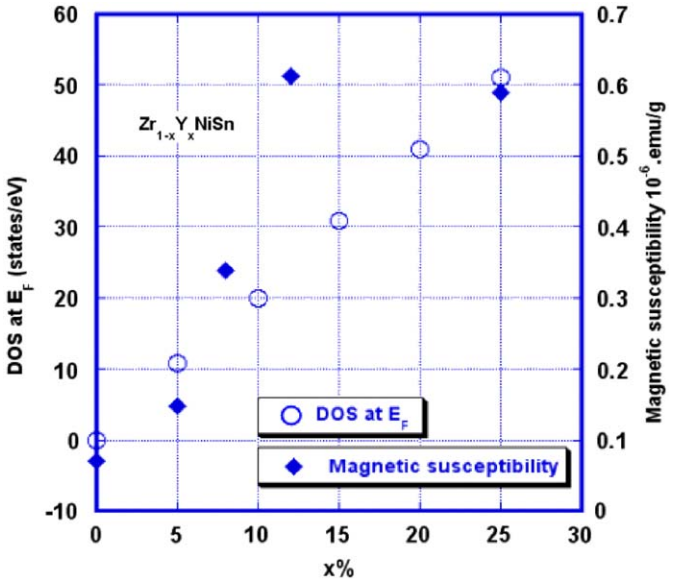

Fig. 9. Behavior of the calculated DOS at Fermi level and the measured magnetic susceptibility versus Y content.

(Fig. 9) that can be considered as the main physical cause of the observed magnetic susceptibility increase, since this physical parameter is proportional to the density of states at the Fermi level in Pauli paramagnet materials. The maximum of static magnetic susceptibility for x=0.1–0.12, not predicted by calculations, is explained in terms of the high magnetic measurement sensitivity to ferri or ferromagnetic impurities presence. From our experience, an impurity with 0.001% content can be detected whereas the X-ray diffraction sensitivity is limited to 2% content.

It is worth noticing that our calculations are performed with measured lattice parameter versus yttrium concentration for cubic system having atoms on special sites (1/2, 1/2, 1/2), (1/4, 1/4, 14) and (0, 0, 0). Therefore, inter atomic distances change are included in calculations, since these distances are proportional to the lattice parameter. As consequence, when Zr is progressively substituted by Y, both charge change and the size effect of Zr/Y are included in calculations that exhibit a continued Fermi level shift towards lower energies

5. Conclusion

Both approaches experimental and calculations point to the same conclusions. Resisitivity and thermopower measurements assert that doping of ZrNiSn based compound by the Y as acceptor impurity induces the insulator–metal transition and leads the *S* value sign reverse. In addition, Pauli paramagnetic character for $Zr_{1-x}Y_xNiSn$ solid solution sample is evidenced by magnetic susceptibility measurements. Results from density of states calculations based on the FPLO method confirm all experimental data assertions and mainly the Seebeck coefficient change when substitution is undertaken.

References

[1] F.G. Aliev, N.B. Brandt, V.V. Moshchalkov, V.V. Kozyrkov, R.V. Skolozdra, A.I. Belogorokhov, Z. Phys. B Condens. Matter 75 (1989) 167.
[2] C. Uher, J. Yang, S. Hu, D.T. Morelli, G.P. Meisner, Phys. Rev. B. 59 (1999) 8615.
[3] H. Hohl, A.P. Ramirez, C. Goldman, G. Ernst, B. Wölfing, E. Buchert, J. Phys. Condens. Matter 11 (1999) 1698.

[4] Yu. Stadnyk, V.A. Romaka, Yu. Gorelenko, L.P. Romaka, D. Fruchart, V.F. Chekurin, J. Alloys Compd. 400 (2005) 29.
[5] O.I. Bodak, V.A. Romaka, Yu.V. Stadnyk, L.P. Romaka, Yu.K. Gorelenko, V.F. Chekurin, Phys. Chem. Solid State 6 (2005) 120.
[6] B.I. Shklovskii, A.L. Efros, Electronic Properties of Doped Semiconductors, Springler, Berlin, 1984 388.
[7] K. Koepernik, H. Eschrig, Phys. Rev. B 59 (1999) 1743.
[8] K. Koepernik, B. Velicky, R. Hayn, H. Eschrig, Phys. Rev. B 55 (1997) 5717.
[9] Yu. Stadnyk, V.A. Romaka, M. Shelyapina, Yu. Gorelenko, L. Romaka, D. Fruchart, A. Tkachuk, V. Chekurin, J. Alloys Compd. 421 (2006) 19.
[10] L.P. Romaka, M.G. Shelyapina, Yu.V. Stadnyk, D. Fruchart, E.K. Hlil, V.A. Romaka, J. Alloys Compd. 416 (2006) 46.
[11] L. Romaka, Yu. Stadnyk, A. Horyn, M.G. Shelyapina, V.S. Kasperovich, D. Frucharc, E.K. Hlil, P. Wolfers, J. Alloys Compd. 396 (2005) 64.
[12] Yu.V. Stadnyk, V.A. Romaka, Yu.K. Gorelenko, L.P. Romaka, D. Fruchart, V.F. Chekurin, J. Alloys Compd. 400 (2005) 29.